Catalytic Reduction of Nitrous Oxide by Carbon Monoxide in the Presence of Rhodium Carbonyl and Hydroxide. Evidence for an Electron-transfer and an Oxygen-transfer Mechanism†

June-Der Lee, Woei-Ping Fang, Chen-Shun Li and Chien-Hong Cheng *
Department of Chemistry, National Tsing Hua University, Hsinchu, Taiwan 30043, Republic of China

The kinetics and mechanism of the reduction of N_2O by CO to N_2 and CO_2 catalysed by the $[Rh_2(CO)_4Cl_2]$–KOH–dmso (dimethyl sulphoxide) system were investigated. A first-order dependence of the rate on both P_{N_2O} and the concentration of $[Rh_2(CO)_4Cl_2]$ was established. The activation parameters $\Delta H^‡$ and $\Delta S^‡$ obtained from an Eyring plot are 59.0 kJ mol^{-1} and −149.4 J K^{-1} mol^{-1} respectively. During the course of catalysis $[Rh_2(CO)_4Cl_2]$ was mainly reduced to $[Rh(CO)_4]^-$. Two other rhodium species $[Rh_4(CO)_{11}]^{2-}$ and $[Rh_4(CO)_{11}(N_2O)]^{\cdot 3-}$ were also detected by ultraviolet–visible and EPR spectroscopies, respectively. The reaction of $[Rh(CO)_4]^-$ with N_2O yielding N_2 and CO_2 simultaneously is believed to be the process responsible for the product formation. Isotopic labelling studies suggest that a direct oxygen transfer from N_2O to CO takes place in the observed catalysis. No reaction of $[Rh(CO)_4]^-$ with N_2O and no catalysis occurs if $[Rh_4(CO)_{11}]^{2-}$ is completely absent from the solution. A catalytic cycle including an electron transfer between $[Rh(CO)_4]^-$ and N_2O to give $N_2O^{\cdot -}$, the trapping of this radical by $[Rh_4(CO)_{11}]^{2-}$ to form $[Rh_4(CO)_{11}(N_2O)]^{\cdot 3-}$ and the evolution of CO_2 and N_2 from the latter radical species is proposed to account for the observed catalysis.

In the reduction of nitric oxide by carbon monoxide using metal complexes as catalysts,[1,2] nitrous oxide is usually the only observed nitrogen product.[3,4] Further reduction of this product by carbon monoxide to give N_2 [equation (1)]

$$N_2O + CO \longrightarrow N_2 + CO_2 \quad (1)$$

generally does not proceed using the same catalyst system, although the reaction is overwhelmingly favoured thermodynamically ($\Delta G^\circ = -360.7$ kJ mol^{-1}). In the absence of catalyst, reaction (1) does not proceed at an appreciable rate below 1000 K.[5] To date, most studies of this environmentally important reaction have employed heterogeneous catalysts, typically at elevated temperature.[6]

Nitrous oxide is a rather inert gas[7] and an extremely poor ligand.[8,9] To the best of our knowledge, there is only one well characterised N_2O complex which was found to release the molecule under mild conditions.[10,11] Compared to other nitrogen oxides, nitrous oxide is relatively unreactive towards halogens and alkali metals at room temperature. While little chemistry of N_2O was revealed, the deoxygenation of N_2O by several transition-metal complexes has been reported.[7,8] A catalytic oxidation of PPh_3 by N_2O using a cobalt(I) complex has been observed.[12]

In a previous communication[13] we have shown that $[Rh_2(CO)_4Cl_2]$ in the presence of base is an active catalyst system for the reduction of NO to N_2O and further to N_2 by CO. Further to understand the mechanism of the reduction of N_2O by CO, we have examined the catalyst system in depth including identification of the intermediates, kinetic, EPR and isotopic labelling studies. The results indicate that the reduction of N_2O occurs *via* a direct oxygen-transfer process from N_2O to CO. Moreover it appears to take place through an unusual electron-transfer step which requires the participation of two different rhodium carbonyl anions.

Experimental

Materials.—The following compounds were obtained from the indicated suppliers: $RhCl_3\cdot 3H_2O$ (Strem), KOH, CH_3CO_2K, dmso (Merck), CO, N_2O, CH_4, C_2H_4 (Matheson) and $H_2{}^{18}O$ (20.5 atom % ^{18}O, MSD). Dimethyl sulphoxide (dmso) was dried over calcium hydride prior to use. The compound $[Rh_2(CO)_4Cl_2]$ was prepared according to a literature method.[14]

General Procedures.—Ultraviolet and visible spectra were obtained on a Perkin-Elmer Lambda 5 spectrophotometer, infrared spectra on a Bomen DA 3.002 Fourier-transform spectrometer in 0.10 or 0.50 mm CaF_2 solution cells and EPR spectra on a Bruker 200D-SRC EPR instrument operated in the X band. A Varian Aerograph model 3700 gas chromatograph with a thermal-conductivity detector in conjunction with a Shimadzu model Chromatopac C-R1B microprocessor was employed for quantitative analysis of gas mixtures. A Pressure-Lok gas syringe obtained from Precision Sampling Corp. was employed for gas samplings. Separation of CO and N_2 was achieved on a molecular sieve 5A column, while a Porapak Q column was used to separate CH_4, CO_2, N_2O and C_2H_4. Mass spectral data were obtained on a JEOL JGC-20K/JMS-D100 GC/MS system; the isotopic compositions of CO_2 were obtained by measuring the ratios of the corresponding peak heights. Calibration plots of CO, CO_2 and N_2O were obtained according to the procedure reported previously.[16]

Kinetic Runs.—A reaction vessel (300 cm^3) containing KOH (2.00 g, 3.57×10^{-2} mol) and dmso (20 cm^3) was evacuated and

---

† *Non-SI units employed:* Torr ≈ 133 Pa, G = 10^{-4} T.

Table 1 Effect of P_{N_2O}, P_{CO}, $[Rh_2(CO)_4Cl_2]$, and temperature on the catalytic rate[a]

Run	$10^3[Rh_2(CO)_4Cl_2]$/ mol dm^{-3}	P_{CO}[b]/ Torr	P_{N_2O}[b]/ Torr	T[a]/°C	$10^4\ k_{obs}$[c]/s^{-1}
A	2.57	400	368	86	2.93 ± 0.07
B	2.57	395	340	86	2.93 ± 0.07
C	2.57	400	310	86	2.88 ± 0.08
D	2.57	396	266	86	2.90 ± 0.08
E	2.57	396	182	86	2.93 ± 0.10
F	2.57	304	340	86	2.95 ± 0.07
G	2.57	205	310	86	2.88 ± 0.10
H	4.29	395	340	86	4.48 ± 0.08
I	3.43	400	340	86	3.68 ± 0.10
J	3.00	400	340	86	3.25 ± 0.10
K	2.59	400	336	86	2.95 ± 0.03
L[d]	1.72	400	335	86	2.00 ± 0.12
M	1.69	400	345	86	1.95 ± 0.05
N[d]	1.20	405	345	86	1.40 ± 0.01
O	0.91	400	340	86	1.10 ± 0.02
P	0.82	395	340	86	0.985 ± 0.015
Q	2.57	400	340	74	1.46 ± 0.01
R	2.57	398	340	67	0.935 ± 0.010
S	2.57	400	340	58	0.505 ± 0.003

[a] The reaction conditions are described in the Experimental section; methane was used as the internal standard except otherwise indicated. Temperature deviation was ±0.5 °C. [b] The initial pressure of the gas. [c] The estimated errors for k_{obs} are listed as standard deviations from linear regressions; a 3% error is estimated for each gas pressure measured. [d] Ethylene was used as the internal standard.

Table 2 Observed ^{18}O distribution of the CO_2 product[a]

Run	$[N(PPh_3)_2][Rh(CO)_4]$/ mol dm^{-3}	Solvent	t/min	Mass	
				44	46
U[a]	1.60×10^{-2}	MeCN	1	0.99	0.0
V[b]	1.60×10^{-2}	dmso	1	0.99	0.0
W[c]	CO_2		15	0.85	0.14

[a] The reaction conditions are described in the Experimental section; the temperature for these runs was 28 ± 2 °C. [b] The reaction conditions were the same as in run U except that ^{18}O-enriched KOH (15.1 atom % ^{18}O) (0.1 g) was used to replace ^{18}O-enriched water. [c] Carbon dioxide (32 Torr) was introduced to the reaction flask containing a solution similar to that described in run V except that no $[Rh(CO)_4]^-$ was added.

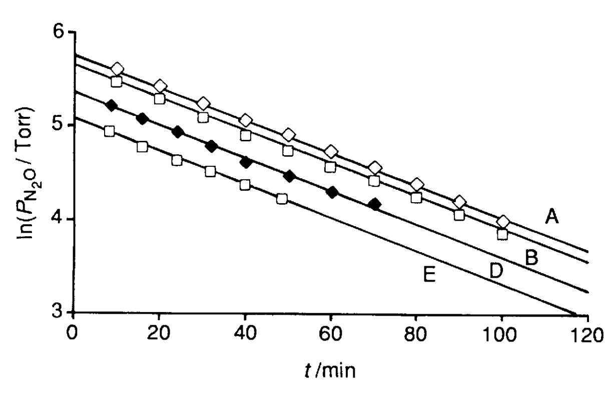

Fig. 1 Plots of ln P_{N_2O} as a function of time (runs A, B, D and E refer to entries in Table 1)

charged with 1 atm (*ca.* 10^5 Pa) CO. The compound $[Rh_2(CO)_4Cl_2]$ (7.71×10^{-5} mol, 0.0300 g) dissolved in dmso (10 cm^3) was syringed into the reaction vessel *via* a septum. The mixture was magnetically stirred at room temperature for 10 h. The vessel was evacuated again and charged with the desired pressure of CO, N_2O and a small amount of methane or ethylene (50–100 Torr) as an internal standard and then immersed in a preheated oil-bath. The solution was stirred magnetically at a constant spinning rate. The gas mixture over the solution was sampled and analysed periodically by gas chromatography (GC). The results and detailed conditions are presented in Table 1 and Figs. 1–3.

EPR Study.—The salt $[N(PPh_3)_2][Rh(CO)_4]$ (0.020 g, 2.66×10^{-5} mol) was added to a EPR tube connected to a vacuum line and to another EPR tube. Into the latter tube was added dimethylformamide (dmf) (1 cm^3). This solution was frozen, evacuated and then thawed. The procedure was repeated twice. To the degassed system was introduced 20 Torr of N_2O. The dmf solution was frozen again and then transferred rapidly as it started to melt to the tube containing $[N(PPh_3)_2]$-$[Rh(CO)_4]$ prior to EPR measurement. The temperature in the cavity was kept at −50 °C. The spectrum observed is shown in Fig. 4.

^{18}O *Isotopic Labelling Studies.*—A solution consisting of $[N(PPh_3)_2][Rh(CO)_4]$ (0.0620 g, 8.23×10^{-5} mol), dmso (5 cm^3), ^{18}O-enriched water (20.5 atom % ^{18}O, 0.10 cm^3) in a flask (30 cm^3) was stirred in the presence of 400 Torr N_2O. The gas mixture over the solution was sampled after the reaction had proceeded for 1 min and was analysed by gas chromatography–mass spectrometry (GC–MS) for the isotopic distribution of carbon dioxide. The results are shown in Table 2.

Results and Discussion

Kinetic Investigations.—The rate of reduction of N_2O by CO catalysed by rhodium carbonyl complexes depends greatly on the base and solvent used.[13] In the present studies, KOH and dmso were chosen as the base and solvent, because under these conditions the catalyst system was observed to be the most effective and the rhodium species present in the catalyst solution are readily identified. However, when KOH was used as the base the CO_2 product was completely absorbed by the base. To avoid a change in basicity of the solution, excess of KOH was employed. Prior to kinetic measurement, it is necessary to pretreat the catalyst solution by stirring it under 1 atm CO to reduce the rhodium complex to the active forms. A slower rate was observed if no pretreatment was performed.

The dependence of the catalytic rate on the partial pressure of N_2O was studied by using solutions consisting of $[Rh_2(CO)_4Cl_2]$ (2.57×10^{-3} mol dm^{-3}), dmso (30 cm^3) and KOH (3.57×10^{-2} mol). Under the conditions, only a small portion of KOH is dissolved in dmso and the concentration of OH^- in the solution is constant throughout the catalysis. While the initial pressure of N_2O was varied from 370 to 180 Torr, a constant partial pressure of CO of 397 ± 3 Torr was introduced into the reaction vessel in each run. As depicted in Fig. 1, plots of ln P_{N_2O} *vs.* time were linear for all runs (only representative runs A, B, D and E are shown) indicative of a first-order dependence on the partial pressure of N_2O. Further support of the relation comes from the slopes of these lines (see Table 1) which are virtually constant within experimental error. All the slopes were determined by least-squares fit of the data. Thus, the rate of the observed catalysis may be expressed

$$\Delta P_{N_2O}/dt = k_{obs}P_{N_2O} \qquad (2)$$

according to equation (2) where $k_{obs} = 2.92 \times 10^{-4}\ s^{-1}$ is the average slope of the lines in Fig. 1.

The observed linear plots shown in Fig. 1 also strongly imply that the rate of catalysis is independent of the partial pressure of CO because a non-linear plot of ln P_{N_2O} *vs.* time should result if the reaction rate also exhibits a dependence on P_{CO}. Further to confirm this notion, two pairs of kinetic runs (B, F and C, G) with each pair employing the same initial partial pressure of N_2O but different partial pressure of CO were performed. As expected, linear plots of ln P_{N_2O} *vs.* time were also obtained.

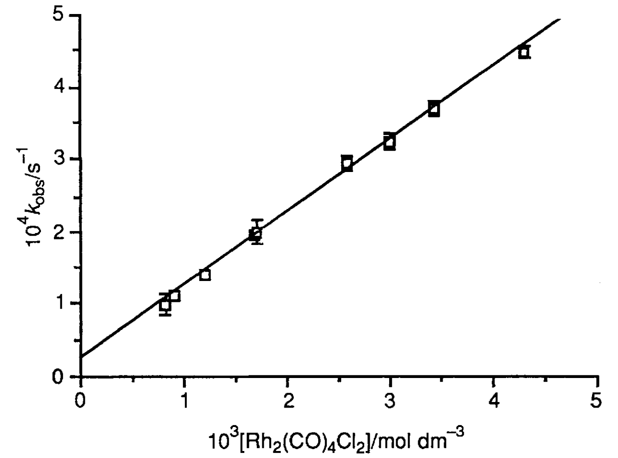

Fig. 2 Effect of the concentration of $[Rh_2(CO)_4Cl_2]$ on k_{obs} at 86 °C

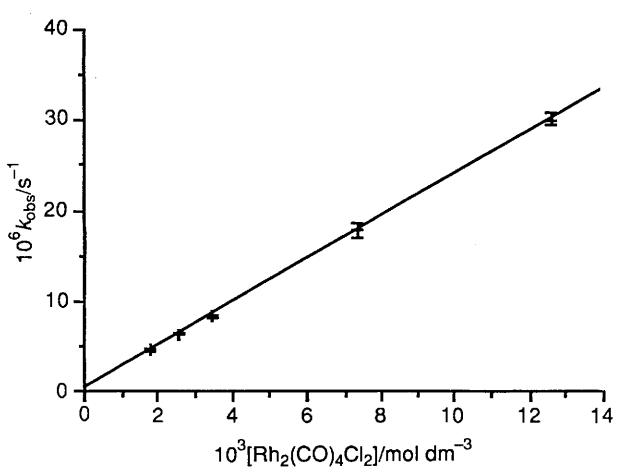

Fig. 3 Effect of the concentration of $[Rh_2(CO)_4Cl_2]$ on k_{obs} at 30 °C

Moreover, the slopes of these plots are the same within experimental error.

To establish the dependence of the reaction rate on the concentration of rhodium catalyst, solutions with various concentrations of $[Rh_2(CO)_4Cl_2]$ (4.29×10^{-3}–8.23×10^{-4} mol dm^{-3}) were employed for kinetic studies. Linear plots of ln P_{N_2O} *vs.* time with different slopes (k_{obs}) were observed (Table 1). A plot of k_{obs} *vs.* the concentration of $[Rh_2(CO)_4Cl_2]$ is linear with a slope of 0.102 ± 0.002 dm^3 mol^{-1} s^{-1} and an intercept of $(2.2 \pm 0.7) \times 10^{-5}$ s^{-1} (Fig. 2). Thus the rate law may be written as in equation (3) where $k = 0.102 \pm 0.002$ dm^3 mol^{-1} s^{-1} and $y^0 = (2.1 \pm 0.6) \times 10^{-4}$ mol dm^{-3}.

$$\Delta P_{N_2O}/dt = k\{[Rh_2(CO)_4Cl_2] + y^0\}P_{N_2O} \qquad (3)$$

The observed non-zero *y* intercept is surprising but can be understood on the basis of the following observations. At the reaction temperature for the catalysis of reaction (1), the dmso–KOH system alone was found to react slowly with N_2O yielding N_2. For example, at an initial N_2O pressure of 350 Torr and in the presence of 2.0 g KOH, the dmso solution (30 cm^3) produced 75 Torr of N_2 at 86 °C in 90 min, while a rhodium catalyst system evolved 238 Torr of N_2 under the same conditions. At the end of the latter catalysis the solution was neutralised by H_2SO_4 to release the absorbed CO_2. A total of 221 Torr CO_2 was detected by GC. The slight excess of N_2 (17 Torr) over CO_2 is attributed to the reaction of dmso–KOH with N_2O during the catalysis. It is notable that less N_2 is formed from the reaction of N_2O with dmso–KOH in the presence of rhodium catalyst than in its absence, due to the competition for N_2O between dmso–KOH and rhodium catalyst. At ambient temperature the reaction of the KOH–dmso system with N_2O is too slow to be detected and a plot of k_{obs} *vs.* $[Rh_2(CO)_4Cl_2]$ as shown in Fig. 3 yields a straight line with essentially a zero intercept (2.92×10^{-7} s^{-1}).

The effect on the catalytic rate of changing the reaction temperature was investigated in the temperature range 86–58 °C. The catalyst system was prepared in a way similar to that of run B. The detailed reaction conditions as well as the rate constants k_{obs} are listed in Table 1 (runs B, Q, R and S). A plot of ln (k_{obs}/T) as a function of $1/T$ yields a straight line. From the intercept and slope the activation parameters were calculated according to the Eyring equation: $\Delta H^\ddagger = 59.0 \pm 0.8$ kJ mol^{-1}, $\Delta S^\ddagger = -149.4 \pm 0.8$ J K^{-1} mol^{-1} and $\Delta G^\ddagger_{298} = 112.5 \pm 0.8$ kJ mol^{-1}.

Identification of Catalytic Intermediates.—In order to understand the mechanism of the observed catalysis, efforts were made to identify the catalyst intermediates by examining the catalyst solution using various spectroscopic methods. During the period of pretreatment of the catalyst system with CO a small portion of the solution was withdrawn periodically and was immediately analysed by Fourier-transform infrared (FTIR) spectroscopy. The results show that $[Rh_2(CO)_4Cl_2]$ was rapidly reduced to a dark green species $[Rh_7(CO)_{16}]^{3-}$ with bands at 1945s, 1811w and 1769m cm^{-1} (ref. 15) in less than 10 min. Further reduction of the rhodium cluster anion to $[Rh_4(CO)_{11}]^{2-}$ (1930 and 1812 cm^{-1})[16] and partially to $[Rh(CO)_4]^-$ (1900 cm^{-1})[17] occurred within 1 h. Finally, a slow reduction of $[Rh_4(CO)_{11}]^{2-}$ to $[Rh(CO)_4]^-$ took place, requiring several hours to complete.

The introduction of N_2O and CO to the pretreated solution followed by heating at the desired temperature (30–86 °C) does not alter the rhodium species in the catalyst solution. The IR spectra indicate the $[Rh(CO)_4]^-$ remains as the major rhodium carbonyl complex detected in the solution. Although other rhodium carbonyl species are too low in concentration to be detected by IR spectroscopy, an ultraviolet–visible spectrum of the orange reacting solution exhibited a weak absorption at 346 nm in addition to the strong absorption band at 265 nm. The former is attributed to the presence of a small concentration of $[Rh_4(CO)_{11}]^{2-}$ in the catalytic solution is evidenced by the observation that $[Rh_4(CO)_{11}]^{2-}$ generated by a known proprocedure also reveals the same absorption band.[16] The strong absorption at 265 nm is from $[Rh(CO)_4]^-$ which is colourless in dmso if no other rhodium carbonyl anion exists.

Chemistry of $[Rh(CO)_4]^-$.—The observation that $[Rh(CO)_4]^-$ appears as the main intermediate during the observed catalysis prompted us to investigate further the properties of this anion. For convenience, the $[N(PPh_3)_2]^+$ salt of the rhodium anion prepared according to a known method[17] was used for these studies. In an experiment using $[N(PPh_3)_2][Rh(CO)_4]$ in KOH–dmso as the catalyst system for reaction (1) the rate of N_2O evolution is essentially the same as that using $[Rh_2(CO)_4Cl_2]$–KOH–dmso. Moreover, the reaction of $[N(PPh_3)_2][Rh(CO)_4]$ with N_2O in dmso at ambient temperature produced 3.7 ± 0.2 mol of N_2, 1.8 ± 0.1 mol of CO_2 and consumed 3.9 ± 0.2 mol of N_2O per mol of $[Rh(CO)]_4{}^-$. (The amount of CO_2 detected in the gas phase is less than expected due to the relatively large solubility of this gas in the dmso solution which is basic.) For comparison, only a trace of N_2 is produced upon treating N_2O with other rhodium anions, $[Rh_7(CO)_{16}]^{3-}$ or $[Rh_4(CO)_{11}]^{2-}$. Surprisingly, a careful examination showed that pure $[Rh(CO)_4]^-$ does not react with N_2O to give N_2 at ambient temperature in the presence of CO. The existence of a small concentration of $[Rh_4(CO)_{11}]^{2-}$ is necessary for the reaction of N_2O with $[Rh(CO)_4]^-$ to proceed. It is worth noting that in a dmso solution of $[N(PPh_3)_2][Rh(CO)_4]$ a small portion of $[Rh(CO)_4]^-$ is readily converted into $[Rh_4(CO)_{11}]^{2-}$ and $[Rh_7(CO)_{16}]^{3-}$ even under strict anaerobic conditions. The rate of conversion increases with the temperature in the presence of excess of CO. However, in the presence of CO, this

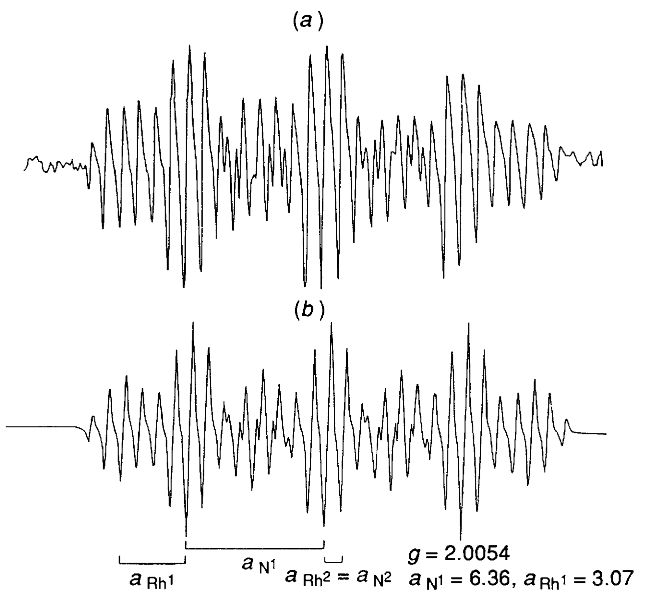

Fig. 4 (*a*) EPR spectrum of a dmf solution containing $[Rh(CO)_4]^-$ and N_2O at −50 °C. (*b*) Simulated EPR spectrum using the parameters given

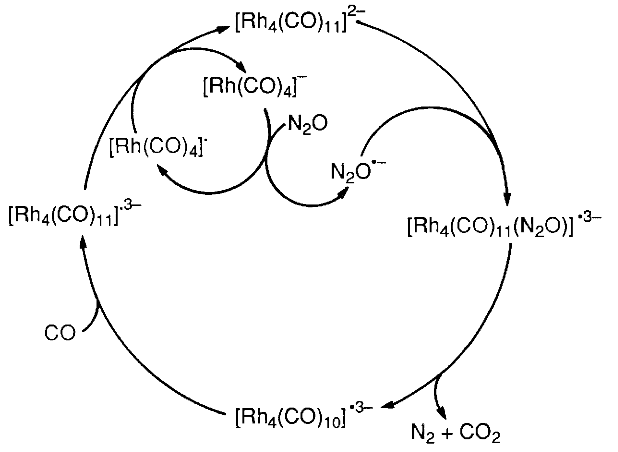

Scheme 1

oxidation of $[Rh(CO)_4]^-$ to rhodium clusters can be prevented at ⩽30 °C.

EPR Studies.—Monitoring the reaction of $[N(PPh_3)_2]$-$[Rh(CO)_4]$ with N_2O in acetonitrile at −50 °C by EPR spectroscopy led to the observation of a complicated EPR signal with g = 2.0054 as shown in Fig. 4(*a*). Rapid evolution of N_2 and CO_2 from the reacting solution and a rapid decrease in the EPR signal were observed as the temperature was raised above −30 °C. However, no EPR signal and no gas evolution were detected from the $[Rh(CO)_4]^-$ solution if CO was present before N_2O was introduced to the EPR tube. The EPR signal was successfully simulated [Fig. 4(*b*)] based on the coupling of the unpaired electron to two non-equivalent nitrogen nuclei ($I = 1$, a_N = 6.36 and 0.75 G), a group of two equivalent rhodium nuclei ($I = \frac{1}{2}$, a_{Rh} = 3.07 G) and another group of two equivalent rhodium nuclei $I = \frac{1}{2}$, a_{Rh} = 0.75 G). A tetrahedral odd-electron species **1** can account for the EPR results. The radical may be viewed as the spin adduct of the $N_2O^{\bullet -}$ radical anion with $[Rh_4(CO)_{11}]^{2-}$ [equation (4)]. The latter presumably arises from the oxidation of $[Rh(CO)_4]^-$ by N_2O or by dmso (see above) and is present in the *[Rh(CO)₄]⁻* solution. It should be noted that in the presence of CO at low temperature the formation of $[Rh_4(CO)_{11}]^{2-}$ from $[Rh(CO)_4]^-$ solution is inhibited and thus no EPR signal may be observed. At this moment, it is not clear from the EPR spectrum how the bridging N_2O group is bonded to the rhodium carbonyl cluster. In structure **1** the central nitrogen of the N_2O moiety is proposed to be bonded to the rhodium atoms, but co-ordination *via* the terminal nitrogen or oxygen atom of N_2O is also in agreement with the EPR results. We favour the bonding shown because the unpaired electron of $N_2O^{\bullet -}$ spends most time on the central nitrogen according to molecular orbital considerations. This radical anion is isoelectronic to the well known NO_2 whose unpaired electron also resides mostly on the central atom. In any case, the observed hyperfine coupling constants of **1** clearly indicate that the odd electron is delocalised on both the nitrogen atoms and the rhodium centres.

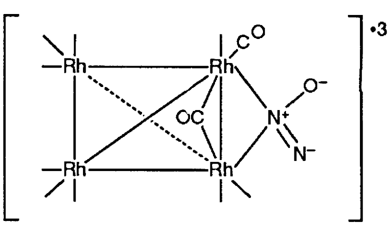

1

Isotopic Labelling Studies.—The reaction of $[N(PPh_3)_2]$-$[Rh(CO)_4]$ with N_2O occurs in strictly dry solvents such as acetonitrile, dmf and dmso. The rate of catalysis of reaction (1) by the rhodium system increases as the amount of water in the solution decreases. These observations strongly indicate that the oxygen of N_2O is transferred to CO to give CO_2 and N_2 in the reaction of $[Rh(CO)_4]^-$ with N_2O and in the catalysis of reaction (1). Further to confirm the oxygen-transfer mechanism, isotopic labelling studies were performed. At the present time we are unable to obtain $N_2{}^{18}O$ for reaction with $[Rh(CO)_4]^-$. Thus, the reaction of $[Rh(CO)_4]^-$ with N_2O in the presence of ^{18}O-enriched water or a water–KOH mixture was carried out. Because, in basic solution, CO_2 in the gas phase was found to undergo oxygen exchange with water (Table 2), only the gas products at the beginning of the reaction were analysed by GC–MS. The results show that essentially no ^{18}O is incorporated into the CO_2 product (Table 2).

Mechanistic Considerations.—On the basis of the foregoing results, a mechanism as shown in equations (4)–(8) and in

$$[Rh(CO)_4]^- + N_2O \underset{k_{-1}}{\overset{k_1}{\rightleftharpoons}} [Rh(CO)_4]^\bullet + N_2O^{\bullet -} \quad (4)$$

$$[Rh_4(CO)_{11}]^{2-} + N_2O^{\bullet -} \xrightarrow{k_2} [Rh_4(CO)_{11}(N_2O)]^{\bullet 3-} \quad (5)$$

$$[Rh_4(CO)_{11}(N_2O)]^{\bullet 3-} \longrightarrow [Rh_4(CO)_{10}]^{\bullet 3-} + N_2 + CO_2 \quad (6)$$

$$[Rh_4(CO)_{10}]^{\bullet 3-} + CO \longrightarrow [Rh_4(CO)_{11}]^{\bullet 3-} \quad (7)$$

$$[Rh_4(CO)_{11}]^{\bullet 3-} + [Rh(CO)_4]^\bullet \longrightarrow [Rh(CO)_4]^- + [Rh_4(CO)_{11}]^{\bullet 2-} \quad (8)$$

Scheme 1 is proposed to account for the observed catalysis. Although rhodium is added in the form of $[Rh_2(CO)_4Cl_2]$ for convenience, in the presence of CO and KOH this rhodium dimer is reduced to carbonyl anions: $[Rh(CO)_4]^-$, $[Rh_4(CO)_{11}]^{2-}$ and an odd-electron species $[Rh_4(CO)_{11}$-$(N_2O)]^{\bullet 3-}$ were observed spectroscopically during the course of catalysis. The mononuclear rhodium carbonyl anion was the main rhodium compound, while the other two species were present only at low concentration or as transient states in the catalyst solution.

The structure of the $Rh(N_2O)$ radical anion and the proposal that it is actively involved in the catalysis of reaction (1) is based on the EPR spectral results and the requirement of both $[Rh(CO)_4]^-$ and $[Rh_4(CO)_{11}]^{2-}$ for the catalysis to proceed. As to how this odd-electron species is formed, we propose that the first step is an electron-transfer reduction of N_2O to $N_2O^{\bullet -}$ by $[Rh(CO)_4]^-$ [equation (4)], in view of the fact that $[Rh(CO)_4]^-$ is the main and most reducing rhodium species. Although the $N_2O^{\bullet -}$ radical is not detected in the present catalysis, presumably due to the low equilibrium concentration and the fast trapping process by $[Rh_4(CO)_{11}]^{2-}$, it has been observed previously in γ-irradiated neopentane or carbon disulphide at 77 K.[18,19] Moreover, in the reaction of $[Rh(CO)_4]^-$ with $PhNO_2$, the $PhNO_2^{\bullet -}$ radical anion is clearly observed[20] further supporting the notion that $[Rh(CO)_4]^-$ readily undergoes one-electron oxidation.

As $N_2O^{\bullet -}$ is trapped by $[Rh_4(CO)_{11}]^{2-}$, back donation from rhodium atoms to N_2O further increases the basicity of the oxygen atom in the N_2O moiety. Thus, attack of the oxygen atom of N_2O at a CO ligand in the radical should occur readily leading to simultaneous evolution of CO_2 and N_2. This interligand oxygen-transfer reaction accounts for the observation of a direct oxygen transfer from N_2O to CO. It is well known that co-ordinated NO_2^-, which is similar to $N_2O^{\bullet -}$ in structure, may also directly transfer one oxygen to a CO ligand.[21–23] However, in the closely related reduction of NO by CO to N_2O and CO_2 catalysed by soluble metal complexes the oxygen in NO does not transfer directly to CO. At least one of the oxygen atoms in CO_2 originates from water.[24]

During the course of catalysis, a steady-state condition is established and all of the rhodium species and $N_2O^{\bullet -}$ in the catalytic solution are present at steady-state concentrations. Application of the steady-state approximation to equations (4)–(8) leads to the rate law (9). When $k_2[Rh_4(CO)_{11}{}^{2-}] \gg k_{-1}[Rh(CO)_4{}^{\bullet}]$, the equation is reduced to (10) or (11). Because

$$-\Delta P_{N_2O}/dt = k_1k_2P_{N_2O}[Rh(CO)_4{}^-][Rh_4(CO)_{11}{}^{2-}]/\{k_{-1}[Rh(CO)_4{}^{\bullet}] + k_2[Rh_4(CO)_{11}{}^{2-}]\} \quad (9)$$

$$-\Delta P_{N_2O}/dt = k_1[Rh(CO)_4{}^-]P_{N_2O} \quad (10)$$

$$= k_1[Rh]_tP_{N_2O} \quad (11)$$

$[Rh(CO)_4]^-$ is the major rhodium species, its concentration is essentially the same as the total concentration of the rhodium carbonyl species. Thus, the expression is quantitatively in agreement with the kinetic experiments which show that the rate of consumption of N_2O is first order in the rhodium concentration and first order in the partial pressure of N_2O. While the concentration of $[Rh_4(CO)_{11}]^{2-}$ does not affect the rate of catalysis under the conditions of the kinetic studies, the rate law also predicts that in the complete absence of this rhodium carbonyl anion no catalysis would occur. This was shown to be true experimentally. Through this kinetic analysis, it is clear that the electron-transfer reaction of $[Rh(CO)_4]^-$ with N_2O should be the rate-limiting step. The large negative entropy of activation, -149.4 J K^{-1} mol^{-1}, for the observed catalysis is in accordance with a rate-limiting reaction between a metal complex and a gas reactant for which the entropy decreases greatly as it is dissolved in solution.

An alternative mechanism for the observed catalysis including a direct attack of $[Rh(CO)_4]^-$ at the central nitrogen of N_2O to give a $[Rh(CO)_4(N_2O)]^-$ adduct followed by an oxygen transfer from the co-ordinated N_2O to CO to yield the gas products also agrees well with the observed kinetics and isotopic labelling studies, but it cannot account for the requirement of $[Rh_4(CO)_{11}]^{2-}$ and the observation of the $[Rh_4(CO)_{11}(N_2O)]^{\bullet 3-}$ radical.

Conclusion

The results of the foregoing studies strongly suggest the involvement of three observed rhodium carbonyl anions, $[Rh(CO)_4]^-$, $[Rh_4(CO)_{11}]^{2-}$ and $[Rh_4(CO)_{11}(N_2O)]^{\bullet 3-}$ in the catalysis of reaction (1). An electron transfer between $[Rh(CO)_4]^-$ and N_2O to give $N_2O^{\bullet -}$ and the co-ordination of this radical to $[Rh_4(CO)_{11}]^{2-}$ prior to N_2 and CO_2 evolution is indicated from these results. The requirement of an electron-transfer step and the co-ordination of the radical is likely related to the great inertness of N_2O. The former step increases the electron density of the N_2O moiety and makes possible its co-ordination to a metal carbonyl and its further reaction with the co-ordinated CO group. Unlike the reduction of NO by CO catalysed by soluble metal complexes, a direct oxygen transfer from N_2O to CO is involved in the present catalysis.

Acknowledgements

We thank the National Science Council of the Republic of China for support of this work.

References

1 (*a*) J. Reed and R. Eisenberg, *Science*, 1974, **184**, 568; (*b*) C. D. Meyer and R. Eisenberg, *J. Am. Chem. Soc.*, 1976, **98**, 1346.
2 B. L. Haymore and J. A. Ibers, *J. Am. Chem. Soc.*, 1974, **96**, 3325; J. A. Kaduk, T. H. Tulip, J. R. Budge and J. A. Ibers, *J. Mol. Catal.*, 1981, **12**, 239.
3 M. Kubota, K. J. Evans, C. A. Koerntgen and J. C. Marsters, jun., *J. Am. Chem. Soc.*, 1978, **100**, 342; *J. Mol. Catal.*, 1980, **7**, 481.
4 K. S. Sun and C. H. Cheng, *J. Chem. Soc., Chem. Commun.*, 1988, 209.
5 H. Lolrat, F. Caralp and M. Destriau, *J. Phys. Chem.*, 1983, **87**, 2455; M. C. Lin and S. H. Bauer, *J. Chem. Phys.*, 1969, **50**, 3377.
6 M. Kobayashi and H. Takegami, *J. Chem. Soc., Faraday Trans. 1*, 1984, **80**, 1221; G. L. Vogler, X. Z. Jiang, J. A. Dumesic and R. J. Madon, *J. Mol. Catal.*, 1984, **89**, 116; S. Akbar and R. W. Joyner, *J. Chem. Soc., Faraday Trans. 1*, 1981, **77**, 803; C. Angeletti, A. Cimino and V. Indovina, *J. Chem. Soc., Faraday Trans. 1*, 1981, **77**, 641; R. Schleppy, jun. and Y. T. Shah, *Ind. Eng. Chem., Prod. Res. Dev.*, 1977, **16**, 47.
7 R. G. S. Banks, R. J. Henderson and J. M. Pratt, *Chem. Commun.*, 1967, 387.
8 F. Bottomley, I. J. B. Lin and M. Mukaida, *J. Am. Chem. Soc.*, 1980, **102**, 5238.
9 M. L. H. Green and C. R. Lucas, *J. Chem. Soc., Dalton Trans.*, 1972, 1000.
10 F. Bottomley and J. R. Crawford, *J. Am. Chem. Soc.*, 1972, **94**, 9092; A. A. Diamantis, G. J. Sparrow, M. R. Snow and T. C. Norman, *Aust. J. Chem.*, 1975, **28**, 1231.
11 F. Bottomley and W. V. F. Books, *Inorg. Chem.*, 1977, **16**, 501.
12 A. Yamamoto, S. Kiazume, L. S. Pu and S. Ikeda, *J. Am. Chem. Soc.*, 1971, **93**, 371.
13 W. P. Fang and C. H. Cheng, *J. Chem. Soc., Chem. Commun.*, 1986, 503.
14 J. A. McCleverty and G. Wilkinson, *Inorg. Synth.*, 1966, **8**, 211.
15 V. G. Albano, G. Ciani, S. Martinengo, P. Chini and G. Giordano, *J. Organomet. Chem.*, 1975, **88**, 381.
16 S. Martinengo, A. Fumagalli, P. Chini, G. V. Albano and G. Giani, *J. Organomet. Chem.*, 1976, **116**, 333.
17 P. Chini and S. Martinengo, *Inorg. Chim. Acta*, 1969, **3**, 21; J. L. Vidal and W. E. Walker, *Inorg. Chem.*, 1981, **20**, 249.
18 S. P. Mishra and M. C. R. Symons, *J. Chem. Soc., Chem. Commun.*, 1972, 510.
19 J. Lin and F. Williams, *J. Phys. Chem*, 1968, **72**, 3707.
20 P. H. Liu and C. H. Cheng, unpublished work.
21 D. T. Doughty, G. Gordon and R. P. Stewart, jun., *J. Am. Chem. Soc.*, 1979, **101**, 2645.
22 D. T. Doughty, R. P. Stewart, jun. and G. Gordon, *J. Am. Chem. Soc.*, 1981, **103**, 3388.
23 J. Kriege-Simondsen, T. D. Bailey and R. D. Feltham, *Inorg. Chem.*, 1983, **22**, 3318.
24 D. E. Hendridsen and R. Eisenberg, *J. Am. Chem. Soc.*, 1976, **98**, 4662.

Received 17*th December* 1990; *Paper* 0/05655C